Adaptive Building Load Control to Enable High Penetration of Solar Photovoltaic Generation

Jin Dong, Mohammed M. Olama, Teja Kuruganti, James Nutaro, Yaosuo Xue, Isha Sharma,
Oak Ridge National Laboratory
Oak Ridge, TN 37831 USA
Email: {dongj,olamahussemm,kurugantipv, nutarojj,xuey,sharmai}@ornl.gov

Seddik M. Djouadi
Dept. of Electrical Engineering and Computer Science
The University of Tennessee
Knoxville, TN 37996 USA
Email: mdjouadi@utk.edu

***Abstract*—This paper investigates the use of a collection of dispatchable heating, ventilation and air conditioning (HVAC) loads to absorb the slow (low-frequency) fluctuations in solar photovoltaic (PV) generation. We find the optimal number of aggregated HVAC loads that offset fluctuations in PV power using power-frequency analysis. To guarantee quality of service, in a fleet of residential/commercial buildings, a quadratic optimization problem is formulated to compute the optimal schedule for a given set of HVAC loads, while maintaining occupants comfort and PV generation constraints. The proposed mechanism not only minimizes the tracking error between PV generation and total consumption, but also significantly reduces the capacity of the required energy storage devices (ESD) such as batteries and fly-wheels. Simulation results show that the proposed mechanism is able to achieve good PV tracking performance as well as obtain a minimal ESD capacity. We show that most of the renewable generation can be consumed locally through an intelligent coordination of HVAC loads that minimizes the impact on the grid and reduces the need for large capacity of ESD.**

***Index Terms*—Building and home automation, energy storage, optimization, advanced and renewable energy technologies, solar photovoltaic power, HVAC.**

I. Introduction

Electric power producers are shifting from using fossil fuels to renewable sources (RES) to generate electricity. RES are expected to account for approximately 24% of new generation capacity by 2040, and are expected to consist predominantly of wind and solar power [1]. Considering intermittent, uncertain and uncontrollable nature of wind and PV generation, the vast integration of large amount of renewable generation would cause output variability and put significant stress on the balance of electric grids. These unwanted characteristics pose technical challenges to regional grid operators and distribution utilities maintaining network frequency and voltage stability [2], [3]. In order to address these challenges, demand side control presents a novel and viable way to assist in managing the balance between supply and demand in the power grid. The massive power consumption and enormous thermal storage enable heating, ventilation and air conditioning (HVAC) systems as a great flexible resource for this kind of demand side service.

This manuscript has been authored by UT-Battelle, LLC under Contract No. DE-AC05-00OR22725 with the U.S. Department of Energy. The United States Government retains and the publisher, by accepting the article for publication, acknowledges that the United States Government retains a non-exclusive, paid-up, irrevocable, world-wide license to publish or reproduce the published form of this manuscript, or allow others to do so, for United States Government purposes. The Department of Energy will provide public access to these results of federally sponsored research in accordance with the DOE Public Access Plan (http://energy.gov/downloads/doe-public-access-plan).

Many researchers have looked towards thermostatically controlled loads (TCLs) to provide demand side services. HVAC systems together with building thermal mass, as the main type of power consumption, can significantly affect the building cooling load due to their considerable capacities and resistances that may be used for demand dispatch. A number of research studies have been conducted to investigate the performance and effects of demand response using HVAC systems (see [4]–[6]). Overall, even with all these referenced works, there is still immense need to gain a deeper understanding of the availability and flexibility of HVAC load. The work in [7] presented a methodology to enumerate the flexibility of thermostatically controlled appliances. Meanwhile, using HVAC systems to provide ancillary services have gained a lot of attention (see [8]–[10]).

The authors of [11] have proposed the idea of initially decomposing the regulation signal into different frequency bands, and conducting demand dispatch corresponding to the matching frequency. Specifically, in order to help offset volatility caused by wind generation, they claim to use fans in HVACs to provide high frequency demand side services, while water pumps contribute to low frequency. Along this line, we did some preliminary analysis for the frequency of PV generation [12]. Through the obtained power spectrum density (PSD), we found out that the dominating frequencies of PV generation lie below 10^{-3} Hz, which is consistent with [11]. Moreover, it is challenging to directly manipulate fan speeds of HVAC systems under current infrastructure, especially for residential houses. No need to mention water pumps are not widely installed across the nation as HVACs, which greatly limits its application scenario. Therefore, we propose a simple and straight forward solution, which is to utilize existing HVAC systems inside residential houses.

The key idea of this paper is to utilize this low frequency HVAC loads to absorb solar fluctuation in the same frequency band. It should be mentioned that, this hybrid battery storage

978-1-5386-2212-4/17/$31.00 ©2017 IEEE

idea has been studied in [13] to smooth wind power generation based on wavelet decomposition method. More recently, [14] talks about using battery-supercapacitor hybrid energy storage system to release the dynamic stress from PV generation.

The main contributions of this paper are as follows. We attempt to shape HVAC loads to track PV generation profile, as well as to minimize the size of energy storage devices (ESD). To guarantee quality of service (QoS) in a fleet of residential buildings, a quadratic optimization problem is formulated to compute the optimal schedule of the HVAC loads subject to temperature comfort band and available PV generation. Compared with existing literature, a more practical HVAC model is considered in the proposed mechanism.

The remainder of this paper is organized as follows. Section II introduces a physics-based model of a single HVAC and a preliminary result for frequency analysis. Section III then derives an optimization formulation for aggregated HVAC loads. Section IV presents the simulation results to validate the tracking performance using a set of real temperature and solar power data. Finally, Section V summarizes the paper and presents the conclusions.

II. System Modeling

A. HVAC Model

In this section, we describe the model used in this work and formulate the problem. The system model was proposed in [15] and employed in [16], [17]. Consider the following continuous-time linear time invariant (LTI) system based on the dynamics of the room temperature, interior-wall surface temperature, and exterior-wall core temperature:

$$\begin{aligned}
\dot{t}_1 &= \tfrac{1}{C_1}[(K_1+K_2)(t_2-t_1)+K_5(t_3-t_1)+K_3(\delta_1-t_1)+u_h \\
&\quad +u_c+\delta_2+\delta_3] \\
\dot{t}_2 &= \tfrac{1}{C_2}[(K_1+K_2)(t_1-t_2)+\delta_2] \\
\dot{t}_3 &= \tfrac{1}{C_3}[K_5(t_1-t_3)+K_4(\delta_1-t_3)]
\end{aligned}$$

where the parameters used in the above model are defined as:

Variables	Definition
t_1	room air temperature [$^\circ F$]
t_2	interior-wall surface temperature [$^\circ$ F]
t_3	exterior-wall core temperature [$^\circ$ F]
u_h	heating power (≥ 0) [kW]
u_c	cooling power (≤ 0) [kW]
δ_1	outside air temperature [$^\circ$ F]
δ_2	solar radiation [kW]
δ_3	internal heat sources [kW]

TABLE I: Parameter definition

All the other variables are constants. The system states are the room air temperature t_1, interior wall surface temperature t_2, and exterior wall core temperature t_3. The control signals u_h and u_c represent heating and cooling power, and they can be combined as one variable $u = u_h + u_c$ because heating and cooling are not simultaneous. For more details about this model, please refer to [15], [16].

Then the thermal model for each individual building is give in state-space form as:

$$\dot{X} = AX + BU + GV \tag{1}$$

where (using parameters defined in Tab. I)

- States $X = [t_1, t_2, t_3]$,
- Inputs $U = [u_c]$,
- Disturbances $V = [\delta_1, \delta_2, \delta_3]$.

It should be mentioned that we are doing summer cooling case only in this paper. State-space matrices A, B, G can be obtained for any given building, and disturbance V is recorded for that specific location.

B. Frequency Response Validation

Spectral analysis of solar PV power output is required to better understand its frequency content and, therefore, optimally assign the different building loads to the appropriate frequency bands (time scales). Fig. 1 shows the frequency domain of a typical summer day of solar PV power output collected from PV cells located on the roof of our Lab. It is observed from Fig. 1 that the cutoff frequency of the low frequency content is about 10^{-3} Hz ($\approx$ 16.7minutes), which contributes to over 98% of the total PV generation. This is a promising finding such that we can aggregate appropriate number of HVACs to generate a matching consumption profile with the same time scale.

Detailed frequency spectrum analysis of PV generation is beyond the scope of this paper. Interested readers can refer to [12] for more details.

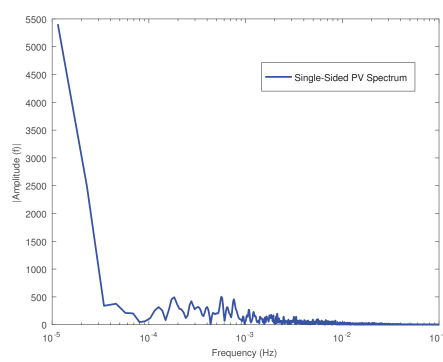

Fig. 1: Spectrum of PV generation

In the sequel, we will investigate whether it is possible to generate a similar power consumption profile with the same frequency by aggregating HVAC loads only. More importantly, an optimal scheduling framework is proposed to dispatch HVAC loads without affecting occupants' comfort.

III. Optimization Problem Formulation

In this studied summer cooling scenario, the thermostat setting point we choose is $26^\circ C$. And a $\pm 2^\circ C$ comfort band is allowed. To make the total power consumption track the available power generation from solar panel, the controller has the freedom to fluctuate temperature inside this comfort band.

We consider the problem where indoor temperature t_1 is required to remain within certain bounds of a constant deadband in the presence of the disturbance vector V. Moreover, we can assign set-points for t_1, but without any other constraints on t_2 and t_3. Thus, we can regulate the output error $e_k := x_k - x_r$ at each time step k, where x_r is the setpoint vector of x.

We aim at minimizing the error e to keep the temperature t_1 close to the desired value. We also require the total control inputs U_{sum} to follow given PV generation P_{PV} signal, i.e.,

$$U_{sum}(t) := \sum_{j=1}^{N_s} u_j(t) \approx P_{PV}(t), \tag{2}$$

where N_s denotes total number of HVAC units.

Thus, our objective is to find for the building system, the M time step control sequences $\{u_0, \cdots, u_{M-1}\}$, where $u_i := u(t_i)$, $i = 0, \cdots, M$; M is an integer, $t_i = i\Delta T$, and $\triangle T$ is the sampling period; and corresponding state sequence $\{x_0, \cdots, x_{M-1}\}$ and error sequence $\{e_0, \cdots, e_{M-1}\}$.

A. Cost Functions

Problem 3.1: If we denote the difference between total control signal and PV signal for each time step k as

$$J_u(k) = \left(\sum_{j=1}^{N_s} (u_j(k)) - P_{PV}(k)\right)' R \left(\sum_{j=1}^{N_s} (u_j(k)) - P_{PV}(k)\right) \tag{3}$$

We consider the difference between total control signal and PV signal together with state deviation.

$$J_1 = \sum_{k=1}^{N_p} \{(x(k) - x_{ref})' Q (x(k) - x_{ref}) + J_u(k)\}, \tag{4}$$

where N_p represents the prediction horizon with $Q \succcurlyeq 0, R \succ 0$ being compatible dimensional matrices. Accordingly, $u_j(k)$ means control action taken for j_{th} building at k_{th} time interval.

Problem 3.2: Furthermore, we may also hope to use as less power as we can to save energy. So we consider the control inputs as a cost in the cost function.

$$J_2 = J_1 + \sum_{k=1}^{N_p} U_k' R_2 U_k. \tag{5}$$

where U_k aligns control actions for all the buildings at time step k in a vector representation.

B. Constraints

We have both states and control inputs constraints in this problem. Since we have three states for each building, we set

$$x_{min} = [24 \quad 0 \quad 0]', \tag{6}$$
$$x_{max} = [28 \quad 50 \quad 50]'; \tag{7}$$

Then for the control input $u \in [0, 1]$. Notice here, 0 means off, and 1 means 1 kW in our model.

After defining constraints for states and inputs of each building, we can easily aggregate them for multiple buildings. Therefore, we have

$$X_{min} = [x_{min}; x_{min}; \cdots]; \quad X_{max} = [x_{max}; x_{max}; \cdots]; \tag{8}$$
$$U_{min} = [0; 0; \cdots]; \quad U_{max} = [1; 1; \cdots]. \tag{9}$$

In addition, we have one more regulation requirement for U_{sum} in (2). Obviously, this turns out to be a linear quadratic programming problem which can be solved by any commercial solver.

Remark 3.3: Once the constraints and objective function have been generated, the optimization problem generated by both Problem 3.1 and 3.2 can be solved as a quadratic programming problem with the control variables U (and the initial state).

IV. CASE STUDIES

This section presents a numerical example to validate our proposed adaptive building load control strategy. We consider a central coordinator that collects total PV generation, and allocates energy to a group of HVAC loads to minimize difference between total consumption and PV generation. Due to space limitation, we only show the results using a standard summer day PV profile. For the other PV generation profiles with different season and sizes, similar results are achieved and will be reported in an extended journal version. It is worth mentioning that terminal simulation time is $T = 96$ for a whole day, which means 15 mins per time step for all the following simulations. Both PV generation and weather profiles are picked for the same day from a local station. All numerical simulations are coded in MATLAB and the quadratic programming (4) is solved using Gurobi [18] through the YALMIP interface [19]. The running time is about 5 seconds on a 2.66 GHz Windows-based laptop with 16 G bytes of RAM.

A. Tracking Performance

The simulation results for indoor temperatures and tracking performances are shown in Fig. 2 - 5 for 20, 30, 40, 50 buildings, respectively. In all the figures, the left hand side in each figure depicts the indoor temperatures for each building (identical buildings with different initial points) under this building load control strategy. The right hand side of Fig. 2 - 5 shows the tracking performance corresponding to a certain number of aggregated buildings. Recall the objective of this paper is to track the PV generation without deviating indoor temperature out of a bound. So both these two variables are key to our design, henceforth, they are provided in Fig. 2 - 5.

It can be seen from Fig. 2 that there barely exists any tracking, even with the presence of maximum power consumption to maintain coolest temperature. Some tracking instances appear in Fig. 3 with 30 buildings, while missing some peaks even with maximum power consumption to maintain coolest temperature in some intervals. Good tracking results are obtained in Fig. 4 with perfect number of buildings, as well as missing some peaks and valleys when hitting temperature bounds (after maximizing temperature flexibility). Tracking performance deteriorates again after increasing the number of building to 50 in Fig. 5, which indicates 50 is too large for this solar profile since it is not tracking well when hitting temperature bounds. In other words, although perfect tracking is not guaranteed all the time, correct control actions are taken to fulfill expected logic.

978-1-5386-2212-4/17/$31.00 ©2017 IEEE

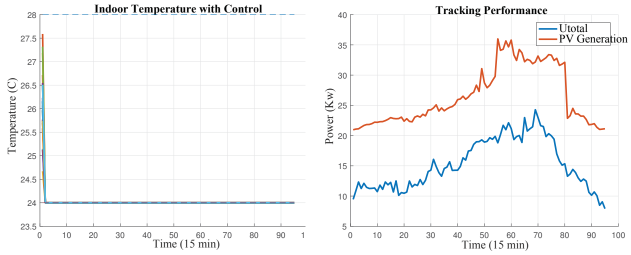

(a) Indoor temperature (b) Tracking PV

Fig. 2: Indoor temperatures and tracking for 20 Buildings

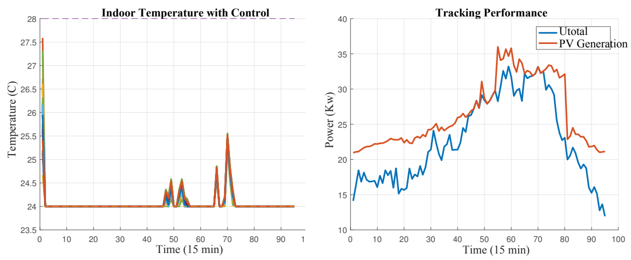

(a) Indoor temperature (b) Tracking PV

Fig. 3: Indoor temperatures and tracking for 30 Buildings

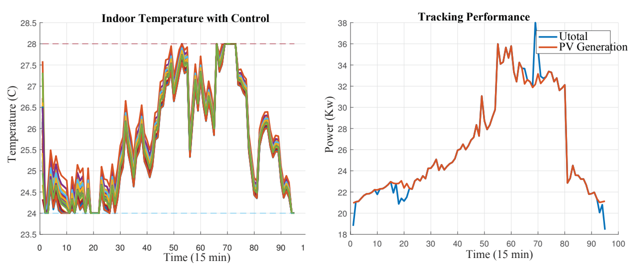

(a) Indoor temperature (b) Tracking PV

Fig. 4: Indoor temperatures and tracking for 40 Buildings

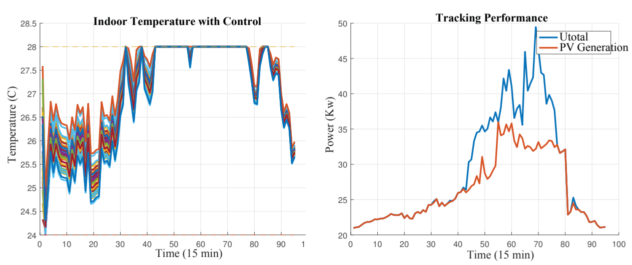

(a) Indoor temperature (b) Tracking PV

Fig. 5: Indoor temperatures and tracking for 50 Buildings

B. Tracking Error

In order to quantify different tracking errors, we compare the Mean Square Error (MSE) for a different number of buildings.

$$MSE = \sqrt{\frac{1}{T}\sum_{t=1}^{T}\left(U_{sum}(t) - P_{pv}(t)\right)^2}, \tag{10}$$

where, $U_{sum}(t)$ is defined in (2).

Through Table II, we see minimum tracking error 2.31 kW is achieved when 40 buildings aggregated. Therefore we can claim the proposed strategy absorbs over 90 % disturbances from PV generation. It should be mentioned that the number of building does play an important role in our algorithm. Tracking error in 20 buildings turns out to be more than five times of that in 40 buildings. The intuitive idea behind this is frequency response of aggregated buildings varies with the number of buildings. This also validates our conjecture at the beginning of this paper, which is low frequency solar response can be absorbed by correct number of aggregated HVACs.

Remark 4.1: Considering the peak PV generation is between 35 $\sim$ 40 kW and the maximum power consumption for each individual HVAC unit is 1 kW, it requires to aggregate 40 buildings to achieve the best tracking performance. Similarly, we run another scenario with 75 $\sim$ 80 kW peak PV generation (not shown in this paper), the optimal number of building is 80. Therefore, we claim the optimal number of building is proportional to peak PV generation.

Cases	Tracking Error (kW)
20 Buildings	11.39
30 Buildings	5.34
40 Buildings	**0.83**
50 Buildings	6.86

TABLE II: Performance Metric for Comparison

C. Energy Storage Size

Though aggregated buildings can provide good tracking performance to the major part of PV generation (especially the low frequency end), some alternative devices are needed to supply the high frequency part. This also validates our finding in Sec. II-B, where high frequency spectrum do exist in Fig. 1 besides the dominating low frequency portion.

Battery storage turns out to be a good candidate since it can provide high frequency tracking compensation. It is a better option than directly controlling fans in HVAC system provided there is no significant modification to existing HVAC units. It should be mentioned that the intuition of this framework is to maximize utilization of aggregated HVAC loads, such that both required size and charge/discharge flow of batteries are minimized. Therefore, installation and maintenance cost for ESD is minimized. In addition, it is more practical and flexible to install the batteries in specific locations.

It is straightforward to compute $P_d(t) := P_{PV}(t) - U_{sum}(t)$ for each time step. If $P_d(t) > 0$, which means PV generation provides more power than total building consumption, then the extra PV generation P_d will be used to charge the battery. Similarly, it will discharge the ESD when $P_d(t) < 0$. $P_d(t)$, i.e., the difference between two trajectories in Fig. 4b is shown in Fig. 6.

If we take the integral of the tracking difference ($P_d(t)$) over time, we can compute the required energy storage size in kWh. Based on Fig. 6, the ESD will be charged first, then discharged during peak time and charged again afterwards. Detailed charge and discharge amounts are listed in Table. III.

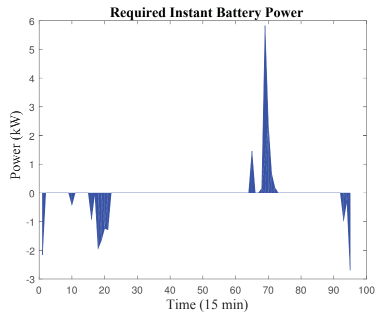

Fig. 6: Required instant ESD power.

Charge/Discharge	Battery Storage (kWh)
Charge (Time step: $0 \sim 30$)	2.13
Discharge (Time step: $60 \sim 80$)	2.67
Charge (Time step: $90 \sim 96$)	0.64
Without HVAC loads	**87.91**

TABLE III: Required Battery Size

Assume the energy storage is half charged at the beginning of the experiment, then a 5 kWh ESD will be more than enough to satisfy the entire charging/discharging requirement to support high frequency response. However, we will need at least 87.91 kWh ESD to store all the PV generation without the proposed HVAC-aided strategy. Hence, we have greatly reduced ESD size which will save a lot of installation and maintenance cost without sacrificing the QoS.

This finding has important implications for accommodating renewable penetration in distribution networks. If most renewable generation can be consumed locally through an intelligent coordination of HVAC loads, their impacts on the grid would be less and the required ESD (either battery or fly-wheel) size can be minimized.

V. CONCLUSIONS

We have studied the ability of a collection of HVAC loads to directly emulate an energy storage device, that is, to track any low frequency fluctuations in PV generation. We obtained the optimal number of aggregated HVAC loads to absorb solar fluctuations in the same frequency band based on frequency analysis. Moreover, the optimal number of buildings is proportional to peak PV generation. To guarantee QoS in a fleet of residential buildings, we formulated a quadratic optimization problem to compute optimal schedule of the HVAC loads considering temperature comfort band and available PV generation. By minimizing the tracking error between PV generation and total consumption, the proposed method also provided the minimum capacity of ESD.

For the future work, we will try to increase the number of building as well as scale of the PV generation to make it more practical in power grid. A distributed optimization algorithm may be needed to overcome scalability issues. We are working on integrating this building-only load with other existing loads in home energy management systems.

ACKNOWLEDGMENT

This material is based upon work supported by the U.S. Department of Energy, Office of Energy Efficiency and Renewable Energy, SunShot National Laboratory Multiyear Partnership (SuNLaMP) program.

REFERENCES

[1] U. DoE, "Annual energy outlook 2014 with projections to 2040," *Washington, DC: US Energy Information Administration, US Department of Energy*, 2014.
[2] Y.-S. Kim, I.-Y. Chung, and S.-I. Moon, "An analysis of variable-speed wind turbine power-control methods with fluctuating wind speed," *Energies*, vol. 6, no. 7, pp. 3323–3338, 2013.
[3] R. Teodorescu, M. Liserre *et al.*, *Grid converters for photovoltaic and wind power systems*. John Wiley & Sons, 2011, vol. 29.
[4] D. T. Nguyen and L. B. Le, "Joint optimization of electric vehicle and home energy scheduling considering user comfort preference," *IEEE Transactions on Smart Grid*, vol. 5, no. 1, pp. 188–199, 2014.
[5] G. Goddard, J. Klose, and S. Backhaus, "Model development and identification for fast demand response in commercial hvac systems," *IEEE Transactions on Smart Grid*, vol. 5, no. 4, pp. 2084–2092, 2014.
[6] A. Saha, M. Kuzlu, and M. Pipattanasomporn, "Demonstration of a home energy management system with smart thermostat control," in *Innovative Smart Grid Technologies (ISGT), 2013 IEEE PES*. IEEE, 2013, pp. 1–8.
[7] M. Heleno, M. A. Matos, and J. P. Lopes, "Availability and flexibility of loads for the provision of reserve," *IEEE Transactions on Smart Grid*, vol. 6, no. 2, pp. 667–674, 2015.
[8] H. Hao, Y. Lin, A. S. Kowli, P. Barooah, and S. Meyn, "Ancillary service to the grid through control of fans in commercial building hvac systems," *IEEE Transactions on smart grid*, vol. 5, no. 4, pp. 2066–2074, 2014.
[9] H. Hao, B. M. Sanandaji, K. Poolla, and T. L. Vincent, "Potentials and economics of residential thermal loads providing regulation reserve," *Energy Policy*, vol. 79, pp. 115–126, 2015.
[10] M. Balandat, F. Oldewurtel, M. Chen, and C. Tomlin, "Contract design for frequency regulation by aggregations of commercial buildings," in *2014 52nd Annual Allerton Conference*. IEEE, 2014, pp. 38–45.
[11] J. Mathias, A. Bušić, and S. Meyn, "Demand dispatch with heterogeneous intelligent loads," *arXiv preprint arXiv:1610.00813*, 2016.
[12] M. Olama, I. Sharma, T. Kuruganti, J. Dong, J. Nutaro, and Y. Xue, "Spectral analytics of solar pv power output to enable high penetration of pv generation," in *2017 IEEE Power & Energy Society General Meeting (Submitted)*, 2017.
[13] T. Kim, H.-j. Moon, D.-h. Kwon, and S.-i. Moon, "A smoothing method for wind power fluctuation using hybrid energy storage," in *Power and Energy Conference at Illinois (PECI), 2015 IEEE*. IEEE, 2015, pp. 1–6.
[14] L. W. Chong, Y. W. Wong, R. K. Rajkumar, and D. Isa, "An optimal control strategy for standalone pv system with battery-supercapacitor hybrid energy storage system," *Journal of Power Sources*, vol. 331, pp. 553–565, 2016.
[15] M. Gwerder and J. Tödtli, "Predictive control for integrated room automation," in *8th REHVA World Congress Clima*, 2005.
[16] F. Oldewurtel, A. Parisio, C. Jones, M. Morari, D. Gyalistras, M. Gwerder, V. Stauch, B. Lehmann, and K. Wirth, "Energy efficient building climate control using stochastic model predictive control and weather predictions," in *Proceedings of the 2010 American control conference (ACC)*. IEEE, 2010, pp. 5100–5105.
[17] X. Ma, J. Dong, S. M. Djouadi, J. J. Nutaro, and T. Kuruganti, "Stochastic control of energy efficient buildings: A semidefinite programming approach," in *2015 IEEE International Conference on Smart Grid Communications (SmartGridComm)*. IEEE, 2015, pp. 780–785.
[18] I. Gurobi Optimization, "Gurobi optimizer reference manual," 2015. [Online]. Available: http://www.gurobi.com
[19] J. Lofberg, "Yalmip: A toolbox for modeling and optimization in matlab," in *Computer Aided Control Systems Design, 2004 IEEE International Symposium on*. IEEE, 2004, pp. 284–289.